CHEMISTRY OF MATERIALS
Communication

Chem. Mater. **2009,** *21,* 2577–2579 2577
DOI:10.1021/cm900291p

Surfactant-Free Organo-Soluble Silica−Titania and Silica Nanoparticles

Abdelhay Aboulaich, Olivier Lorret, Bruno Boury, and P. Hubert Mutin*

Institut Charles Gerhardt Montpellier, UMR5253 CNRS-UM2-ENSCM-UM1, Chimie Moléculaire et Organisation du Solide, Université Montpellier 2, CC1701, 34095 Montpellier Cedex 5, France

Received January 31, 2009
Revised Manuscript Received April 23, 2009

Titania-silica and silica nanoparticles present promising applications in a number of areas including optics, catalysis, composite materials, pigments, bioanalysis and drug-delivery.[1−6] The sol−gel process is recognized as one of the most versatile and cost-effective techniques for the synthesis of unaggregated nanoparticles of controlled size and shape.[7−9]

Thus, silica nanoparticles can be obtained by hydrolysis−condensation of silicon alkoxides in aquo-alcoholic media in the presence of a base, as in the well-known Stöber process.[1,10] In aqueous media, the silica sols are commonly stabilized against aggregation by an electrostatic double layer (electrostatic stabilization).

However, it has been shown that alkaline aqueous conditions are not suitable for the synthesis of homogeneous mixed silica-metal oxides such as SiO_2-TiO_2.[11,12] Furthermore, in order to prevent aggregation in organic solvents, it is necessary to modify the surface of the nanoparticles by adsorption of surfactants or by grafting organosilanes molecules.

Nonhydrolytic (or nonaqueous) sol−gel[13,14] in anhydrous media has become a powerful method for the synthesis of crystalline metal oxide nanoparticles, such as TiO_2, ZrO_2, Fe_3O_4, or $BaTiO_3$.[15,16] In these nonhydrolytic routes, the aggregation is controlled by steric stabilization, which results from the addition of surfactants,[17]or the use of a solvent such as benzyl alcohol,[18] which acts as a capping agent.[16] Although nonhydrolytic sol−gel routes have been successfully used for the synthesis of silica[19] and silica-metal oxide mesoporous xerogels,[12,20,21] they have never been applied to the synthesis of amorphous silica-based nanoparticles.

Here we report a nonhydrolytic synthesis of homogeneous silica−titania and of silica nanoparticles, using a simple route based on the etherolysis and condensation of chloride precursors with diisopropyl ether (eqs 1 and 2). We show that the resulting nanoparticles form stable sols in anhydrous aprotic organic solvents, in the absence of any surfactant or coordinating solvent, and that this unprecedented behavior can be attributed to the unique surface functionality of the nanoparticles. Additionally, the interest in these nanoparticles for the straightforward preparation of polymer nanocomposites and the deposition of nanoparticle monolayers is demonstrated.

$$M-Cl + {}^{i}Pr_2O \rightarrow M-O{}^{i}Pr + {}^{i}PrCl \quad (1)$$

$$M-Cl + M-O{}^{i}Pr \rightarrow M-O-M + {}^{i}PrCl \quad (2)$$

The nanoparticle sols were obtained by heating the chloride precursors diluted in CH_2Cl_2 with a stoichiometric amount of diisopropyl ether in sealed tubes under autogenous pressure. The detailed experimental procedure can be found in the Supporting Information. In the case of the silica particles (denoted NH-Si), the reactions were catalyzed by $ZrCl_4$ (0.5 mol %); in the case of the silica−titania nanoparticles (denoted NH-SiTi), no catalyst was needed, as shown in Scheme 1. Under these conditions, soft gels formed after ~2.5 days for NH-Si or 6 days for NH-SiTi; however, when the reaction was stopped at about 80% of the gel time by cooling the tubes at room temperature, transparent sols were obtained.

^{1}H NMR of the sols indicated that most of the $^{i}Pr_2O$ had reacted and that $^{i}PrCl$ and isopropoxide groups formed. The degree of condensation estimated from the integration of the different signals was about 70−75%.

*Corresponding author. E-mail: mutin@univ-montp2.fr.

(1) Iler, R. K. The Chemistry of Silica; Wiley-VCH: New York, 1979.
(2) Mark, J. E. *Acc. Chem. Res.* **2006**, *39*, 881–888.
(3) Kursawe, M.; Anselmann, R.; Hilarius, V.; Pfaff, G. *J. Sol-Gel Sci. Technol.* **2005**, *33*, 71–74.
(4) Stark, W. J.; Pratsinis, S. E.; Baiker, A. *J. Catal.* **2001**, *203*, 516–524.
(5) Laurent, S.; Forge, D.; Port, M.; Roch, A.; Robic, C.; Vander Elst, L.; Muller, R. N. *Chem. Rev.* **2008**, *108*, 2064–2110.
(6) Barbe, C.; Bartlett, J.; Kong, L.; Finnie, K.; Lin, H. Q.; Larkin, M.; Calleja, S.; Bush, A.; Calleja, G. *Adv. Mater.* **2004**, *16*, 1959–1966.
(7) Brinker, C. J.; Scherer, G. W. Sol−Gel Science: The Physics and Chemistry of Sol−Gel Processing; Academic Press: Boston, MA, 1990.
(8) Shukla, S.; Seal, S. In Synthesis, Funcionalization and Surface Treatment of Nanoparticles; Baraton, M.-I., Ed.; American Scientific Publisher: Stevenson Ranch, CA, 2003; pp 31–−49.
(9) Cushing, B. L.; Kolesnichenko, V. L.; O'Connor, C. J. *Chem. Rev.* **2004**, *104*, 3893–3946.
(10) Stoeber, W.; Fink, A.; Bohn, E. *J. Colloid Interface Sci.* **1968**, *26*, 62–9.
(11) Dutoit, D. C. M.; Schneider, M.; Baiker, A. *J. Catal.* **1995**, *153*, 165–176.
(12) Lafond, V.; Mutin, P. H.; Vioux, A. *Chem. Mater.* **2004**, *16*, 5380–5386.
(13) Vioux, A. *Chem. Mater.* **1997**, *9*, 2292–2299.
(14) Mutin, P. H.; Vioux, A. *Chem. Mater.* **2009**, *21*, 582–596.
(15) Jun, Y.-W.; Choi, J.-S.; Cheon, J. *Angew. Chem., Int. Ed.* **2006**, *45*, 3414–3439.
(16) Garnweitner, G.; Niederberger, M. *J. Am. Ceram. Soc.* **2006**, *89*, 1801–1808.
(17) Trentler, T. J.; Denler, T. E.; Bertone, J. F.; Agrawal, A.; Colvin, V. L. *J. Am. Ceram. Soc.* **1999**, *121*, 1613–1614.
(18) Niederberger, M.; Bartl, M. H.; Stucky, G. D. *J. Am. Chem. Soc.* **2002**, *124*, 13642–13643.
(19) Bourget, L.; Corriu, R. J. P.; Leclercq, D.; Mutin, P. H.; Vioux, A. *J. Non-Cryst. Solids* **1998**, *242*, 81–91.
(20) Andrianainarivelo, M.; Corriu, R. J. P.; Leclercq, D.; Mutin, P. H.; Vioux, A. *J. Mater. Chem.* **1996**, *6*, 1665–1671.
(21) Cojocariu, A. M.; Mutin, P. H.; Dumitriu, E.; Fajula, F.; Vioux, A.; Hulea, V. *Chem. Commun.* **2008**, 5357–5359.

Published on Web 05/13/2009

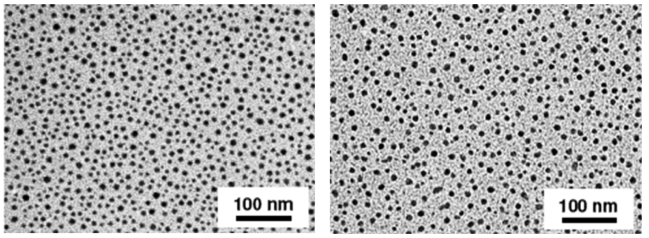

Figure 1. TEM images of NH-Si (left) and NH-SiTi (right) nanoparticles.

Scheme 1. Syntheses of the Nanoparticle Sols

$$SiCl_4 + 2\,{}^{i}Pr_2O \xrightarrow[[ZrCl_4]\ 80\ ^\circ C,\ 2\ d.]{CH_2Cl_2\ (15\ vol.)} \text{NH-Si}$$

$$0.9\,SiCl_4 + 0.1\,TiCl_4 + 2\,{}^{i}Pr_2O \xrightarrow[110\ ^\circ C,\ 5\ d.]{CH_2Cl_2\ (15\ vol.)} \text{NH-SiTi}$$

Table 1. Specific Surface Area, Density, Average Diameter, and Ti and Zr Content of the Non-Hydrolytic Nanoparticles

sample	S_{BET} (m^2g^{-1})	d^a (g cm^{-3})	D^b (nm)	M/(Si + M)^c (%)
NH-Si	320	1.58	11.9	0.7 ± 0.3^d
NH-SiTi	300	1.64	12.2	9.8 ± 0.5^e

[a] Density measured by helium pycnometry. [b] Average diameter $D = 6000/(d \times S_{BET})$. [c] Measured by MEB-EDX. [d] M = Zr. [e] M = Ti.

TEM images of diluted sols evaporated on a grid (Figure 1) showed in both cases the presence of well-dispersed spherical nanoparticles with sizes in the 8−14 nm range. The average diameter of the nanoparticles calculated from their BET specific surface area (see Supporting Information) and their density was in good agreement with the size observed by TEM (Table 1), suggesting that NH-Si and NH-SiTi nanoparticles were nonporous.

In the absence of water, the NH-Si and NH-SiTi sols remained stable for months at room temperature, indicating that the rate of nonhydrolytic condensation (eq 2) is negligible at this temperature. Furthermore, the sols could be concentrated by evaporating the solvent and then redispersed in dry organic solvents such as THF or CH_2Cl_2, leading to unaggregated nanoparticles, as verified by TEM imaging. Dynamic light scattering experiments were done in the case of NH-Si nanoparticles. It was necessary to disperse the particles in a solvent with a high refractive index (chlorobenzene) to have sufficient contrast. A sharp size distribution was obtained (see the Supporting Information), with an average diameter of 10.1 nm, in good agreement with the size determined by TEM.

Both nanoparticles were amorphous to XRD. Elemental analysis of the nanoparticles by EDX indicated that Zr or Ti were incorporated in the nanoparticles (Table 1). In addition, UV−vis spectroscopy indicated that no anatase could be detected at 330 nm in NH-SiTi nanoparticles even after calcination at 500 °C (Figure 2), which demonstrated the homogeneous incorporation of Ti atoms in NH-SiTi.[22] Whereas NH-Si particles were transparent in the 220−800 nm range, the spectrum of NH-SiTi showed an absorption band at 260 nm that corresponds to four-coordinated Ti atoms and a shoulder at 290 nm, suggesting the presence of higher-coordinated Ti atoms.[22] To the best of our knowledge, this is the first example of a sol−gel synthesis of homogeneous, unaggregated SiO_2−TiO_2 nanoparticles.

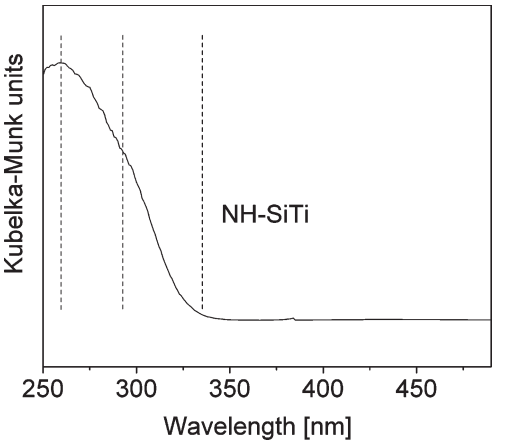

Figure 2. Diffuse reflectance UV−vis spectrum of NH-SiTi nanoparticles.

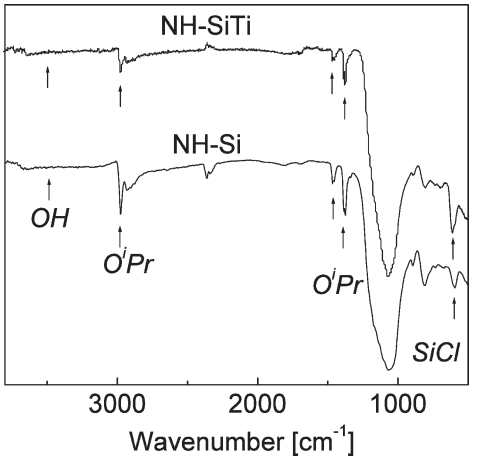

Figure 3. FTIR spectra of NH-Si (bottom) and NH-SiTi (top) nanoparticles.

To rationalize the stability of the nanoparticles, further techniques were used to characterize these systems and more specifically the groups at the surface. Transmission FTIR spectra of the dried nanoparticle (Figure 3) show the absence of hydroxyl groups, which would absorb between 3700 and 3200 cm^{-1}. On the other hand, vibrations at 1375−1385 and 2975 cm^{-1} indicate the presence of ^{i}Pr groups, and a vibration at about 610 cm^{-1} shows the presence of Si−Cl groups.[23,24] The presence of residual Cl and O^{i}Pr groups was confirmed by solid-state ^{29}Si CP-MAS NMR spectroscopy of NH-Si nanoparticles, which showed the presence of $Si(OSi)_{4-x-y}(O^{i}Pr)_yCl_x$ sites (see the Supporting Information).

Thermogravimetric analysis (TGA) of the powders obtained after drying the nanoparticles under vacuum (100 Pa) at 25 °C for 3 h showed weight losses of 30% for NH-SiTi and 32% for NH-Si between 100 and 800 °C

(22) Davis, R. J.; Liu, Z. F. *Chem. Mater.* **1997**, *9*, 2311–2324.
(23) Lang, S. J.; Morrow, B. A. *J. Phys. Chem.* **1994**, *98*, 13314–13318.
(24) Sneh, O.; Wise, M. L.; Ott, A. W.; Okada, L. A.; George, S. M. *Surf. Sci.* **1995**, *334*, 135–152.

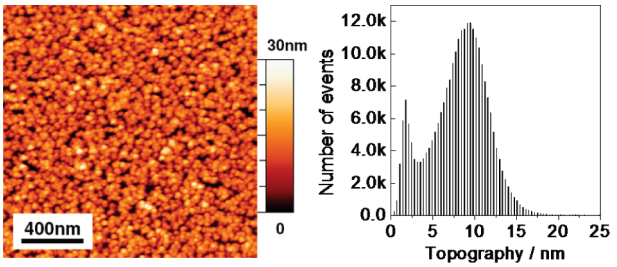

Figure 4. AFM image of a monolayer of NH-Si nanoparticles deposited on an oxidized Si wafer (left) and height distribution (right).

Scheme 2. Deposition of a Nanoparticle Monolayer on a Silicon Wafer by Reaction at Room Temperature of the Cl and O^{i}Pr Surface Groups of the Nanoparticles with the Surface Silanols

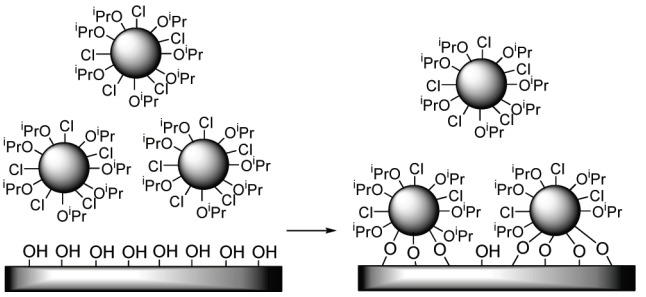

(see the Supporting Information). The degrees of condensation calculated from these weight losses (assuming an equal number of residual O^{i}Pr and Cl groups) were 84% for NH-SiTi and 82% for NH-Si. These values are higher than that estimated from the ^{1}H NMR spectra of the sols (70−75%), suggesting that condensations occurred during the drying treatment.

As a result, the stability of these nanoparticle sols in organic solvents can be ascribed to the nature of the residual groups present at their surface (Cl and O^{i}Pr groups instead of OH groups). These groups render the particles organophilic. In addition, the negligible rate of nonhydrolytic condensations at room temperature makes the sol kinetically stable in the absence of water.

However, Si−Cl and to a lesser extent Si−O^{i}Pr groups are reactive toward nucleophiles, such as water, alcohols, or surface silanols. Thus, immersion of an oxidized Si wafer in a crude nanoparticle sol led to the grafting of the particles to the wafer surface (Scheme 2). AFM images (Figure 4) revealed that in the absence of water, only monolayers of nanoparticles were obtained whatever the immersion time between 30 s and 4 h.

This self-limiting grafting can be explained by the surface chemistry of the nanoparticles: at room temperature and in the absence of water, nanoparticles can bind to the wafer surface by condensation with silanol groups, but cannot bind to each other.

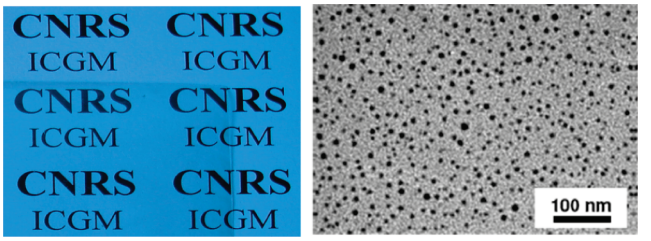

Figure 5. Transparent PMMA film incorporating 7 wt % NH-Si nanoparticles (left) and TEM image of a microtome cut (70 nm thick) (right).

The organophilicity of these nanoparticles makes them compatible with common hydrophobic polymers, such as PVC or PMMA, which allows the straightforward preparation of highly homogeneous organic−inorganic nanocomposites without any surface modification of the particles, whereas conventional hydrophilic nanoparticles have to be modified to avoid aggregation. For instance, PMMA dissolved in CH_2Cl_2 was mixed to a crude NH-Si sol and tape-casting of the resulting viscous solution led after evaporation of the solvent to transparent nanocomposite films, about 200 μm thick. The optical transmission quantified by UV−vis spectroscopy was higher than 94% in all the visible range. The TEM image of a microtome cut (Figure 5) of a PMMA/NH-Si nanocomposite incorporating 7 wt % nanoparticles illustrates the excellent dispersion of the nanoparticles in the polymeric matrix.

In conclusion, the nonhydrolytic reaction of chloride precursors with diisopropyl ether, in the absence of surfactant or coordinating solvent, offers an extremely simple and easily scalable route to silica and homogeneous silica−titania nanoparticles. These particles are terminated by chloride and isopropoxide groups. A whole range of original properties stems from this unique surface chemistry: the nanoparticles are organophilic, they form metastable sols in anhydrous organic solvents, and they can be readily dispersed in hydrophobic polymer matrices without any surface modification. Finally, the nanoparticles covered by reactive chloride and isopropoxide groups can be used as nanobuilding blocks, opening exciting possibilities for the design of nanomaterials. For instance, the particles bind strongly to hydroxylated surfaces, leading to the self-limiting deposition of monolayers.

Supporting Information Available: Experimental details and characterization data for the nanoparticles (PDF). This material is available free of charge via the Internet at http://pubs.acs.org.